ISSN 0016-7029, Geochemistry International, 2007, Vol. 45, No. 1, pp. 62–69. © Pleiades Publishing, Ltd., 2007.
Original Russian Text © S.V. Ikorsky, A.A. Avedisyan, 2007, published in Geokhimiya, 2007, No. 1, pp. 71–78.

Hydrocarbon Gases and Helium Isotopes in the Paleozoic Alkaline–Ultramafic Massifs of the Kola Peninsula

S. V. Ikorsky and A. A. Avedisyan

Geological Institute, Kola Scientific Center, Russian Academy of Sciences,
ul. Fersmana 14, Apatity, Murmansk oblast, 184200 Russia
e-mail: ikorsky@geoksc.apatity.ru

Received April 22, 2005

Abstract—Hydrocarbon gases (HCG) were studied in fluid inclusions from seven alkaline–ultramafic massifs of the Kola Peninsula. All the massifs (Sebljavr, Kovdor, Lesnaya Varaka, Ozernaya Varaka, Vuorijarvi, Turii Peninsula, and Salma) are central-type cratonic intrusions with ages of 360–410 Ma. Previous He isotopic investigations showed that the massifs have high $^3He/^4He$ ratios (up to 3.3×10^{-5}), which are usually higher than the upper mantle value. Similar to He, HCG were extracted by crushing. The HCG were analyzed for CH_4 (main component), C_2H_6, and C_3H_8. A comparison of HCG component contents with He isotope abundances and ratios showed that the HCG were probably not supplied by mantle-derived melts. Their formation during a postmagmatic stage at relatively low temperatures is our favored model.

DOI: 10.1134/S0016702907010053

Interest in hydrocarbon gases from alkaline–ultramafic massifs of the Kola Peninsula is related to the fact that the isotope ratio $^3He/^4He$ of helium trapped in the rocks of the massifs is higher than the modern upper mantle value [1, 2]. The age of the massifs is 360–410 Ma [3]. The highest $^3He/^4He$ ratio of 3.3×10^{-5} was measured in the rocks of the Sebljavr Massif. The estimates of $^3He/^4He$ ratios are 1.12×10^{-5} for the modern upper mantle, 18.2×10^{-5} for the lower mantle, and 1×10^{-8} for the continental crust [4]. The obtained data suggested a genetic relation between the Paleozoic alkaline–ultramafic intrusions of the Kola Peninsula and mantle plume activity [2]. The results of subsequent studies confirmed and justified in more detail the contribution of lower mantle material to the formation of these intrusive complexes [5, 6].

Helium is present in trace amounts in the fluid phase of magmatic melts [7]. However, as an indicator of a genetic link between alkaline–ultramafic intrusions and the mantle, He may bear witness to the mantle origin of other fluid components of alkaline and ultramafic rocks. The components of interest are hydrocarbon gases (HCG), which occur in variable amounts in the rocks of these massifs [8]. The possibility of the presence of hydrocarbons in the mantle was considered in numerous publications. Sugisaki and Mimura [9] suggested that heavy hydrocarbons could occur in the mantle, but they were decomposed to lighter hydrocarbons (ultimately, to methane) during their ascent with mantle magmas in response to a change in P–T conditions. However, there are contrary views. According to thermodynamic calculations, methane-bearing fluids can be formed only at a postmagmatic stage owing to the reaction between H_2 and C under relatively low-temperature conditions [10]. This conclusion was confirmed, in particular, by data on the Khibiny alkaline massif, where rocks with HCG inclusions are mainly confined to the zones of postmagmatic alteration of nepheline syenites [11].

Given the mantle He isotopic signatures of fluid inclusions from these rocks, it is interesting to examine the relations of helium with other components of fluid inclusions, hydrocarbon gases, in order to constrain their genesis. Aliquots for HCG analysis were taken from the same samples in which He measurements were previously made. Similar to the study of He, HCG were extracted from inclusions by crushing in a miniature vibration mill installed in the gas system of a TSVET-102 chromatograph [12]. During He extraction, samples were crushed in evacuated glass ampoules, which were then opened in the gas-loading apparatus of a MI-1201 mass spectrometer [13]. The extent of crushing in these two techniques was nearly the same. As a result, the same 85 samples taken from seven Paleozoic alkaline–ultramafic massifs of the Kola Peninsula were sequentially analyzed for the abundances and isotopic compositions of He and hydrocarbon gases. All these massifs are central-type cratonic intrusions. Their names are given in Table 1, and geological characteristics are available in [14].

HCG were studied in samples taken from main intrusive phases: ultramafic (olivinite and pyroxenite) and alkaline (ijolite–urtite, ijoilite, and melteigite). In the Kovdor and Salma massifs, HCG were also studied in melilite rocks, the genesis of which was supposedly related to postmagamtic processes [14]. Among the

Table 1. Compositions and contents of hydrocarbon gases (HCG) in fluid inclusions in the rocks of the alkaline–ultramafic massifs compared with ^{3}He abundances and He isotope compositions expressed as the R/Ra (^{3}He/^{4}He) ratio

Sample*	Rock (mineral)	HCG, cm^3/g × 10^{-6}			^{3}He, cm^3/g ×10^{-12}	R/Ra** (^{3}He/^{4}He)
		CH_4	C_2H_6	C_3H_8		
Sebljavr massif						
NSB-138/160	Olivinite	9353.0	51.3	0.14	120.9	19.6
Sja-184/80	Olivinite	216.9	3.04	0.21	98.1	11.9
NSB-138/70	Pyroxenite	955.0	5.36	0.24	742.0	23.7
Sja-186/130	Pyroxenite	37.8	0.78	<0.0335	425.0	17.6
Sja-114/65	Pyroxenite	47.8	1.38	0.40	216.0	13.1
Sja-114/7	Pyroxenite	915.4	16.2	0.15	670.5	15.64
Sja-114/55	Pyroxenite	1731.0	25.0	0.49	412	17.43
Sja-114/55-pr	Pyroxene from pyroxenite	1671.6	19.6	0.5	388	17.0
Sja-114/55-mgt	Magnetite from pyroxenite	529.3	16.7	1.1	601	16.0
Kovdor massif						
KR-18-1/126	Olivinite	38.2	0.82	0.15	2.0	8.5
KR-41-1/199	Olivinite	10.7	0.66	0.17	35.0	11.86
KR-55-1/257.8	Olivinite	32.2	0.98	<0.0335	62.0	8.5
KR-59-1/268.1	Olivinite	14.7	0.63	<0.0335	62.3	11.21
KR-62-1/276	Olivinite	19.1	0.54	<0.0335	91.6	10.57
KR-80-1/357.8	Olivinite	45.4	0.66	≤0.0335	109	11.43
KR-133-1/997.3	Olivinite	8.0	0.39	0.07	10.1	5.62
D-52	Olivinite	86.6	0.72	<0.0335	32.1	11.86
KR-35-1/171.4	Pyroxenite	27.5	0.29	<0.0335	239	7.12
KR-5S/152-1598	Pyroxenite	22.3	0.24	<0.0335	146	8.29
KI-21	Pyroxenite	105.5	0.95	0.12	26.5	11.86
KR-193	Ijolite	51.7	1.25	0.37	33.7	4.71
KI-16	Ijolite	33.4	0.94	0.09	116	6.44
KI-22-A	Melilite	390.0	2.0	<0.0335	56.0	10.5
D-54	Melilite	29.9	0.72	0.12	19.4	5.43
GIM-4652	Turjaite	3761.1	13.1	0.30	222	14.05
Lesnaya Varaka massif						
LVM-2nn	Massive mineralized olivinite	314.4	2.5	0.23	10.2	9.86
LVM-2/oL	Olivine from olivinite	29.5	0.95	0.14	1.3	7.86
LVM-2/mgt	Magnetite from olivinite	537.0	3.46	0.17	20.3	11.79
LV-8/117	Ti-magnetite from coarsely banded olivinite	413.9	4.1	0.37	141.1	6.5
GIM-343	Magnetite schlieren	1492.5	28.6	1.27	48.5	3.65
GIM-3287	Barren olivinite	786.0	10.8	0.65	32.3	8.29
GIM-3287/3	Olivinite	601.0	7.8	1.02	50.12	9.5
LV-80/1-pr	Pyroxene from mineralized pyroxenite	5890.0	63.3	0.60	19.7	6.39
LV-80/1-mgt	Magnetite from mineralized pyroxenite	975.0	9.5	0.97	16.0	4.57

Table 1. (Contd.)

Sample*	Rock (mineral)	HCG, $cm^3/g \times 10^{-6}$			^3He, cm^3/g $\times10^{-12}$	R/Ra** ($^3He/^4He$)
		CH_4	C_2H_6	C_3H_8		
Vuorijarvi massif						
25v-229/256.8	Olivinite	11.9	0.27	<0.0335	42.0	4.91
NVV-288/152	Olivinite	10.1	0.12	<0.0335	56.8	11.29
NVV-288/202	Olivinite	11.1	0.12	<0.0335	41.4	8.57
N-426/226	Pyroxenite	16.3	0.5	0.23	170.2	1.9
NVV-95/140	Nepheline pyroxenite	1383.0	39.3	1.0	135	5.66
NVV-307/126	Pyroxenite	2626.8	12.6	0.12	321	10.25
NVV-258/96	Pyroxenite	885.6	4.8	<0.0335	148.2	11.36
NVV-289/325	Ijolite	45.8	4.61	1.41	6.66	3.74
NVV-289/325-1	Ijolite	19.1	1.79	0.51	78.1	2.03
N-417/158.0	Ijolite	14.3	0.15	0.28	187	4.7
NVV-438/102	Ijolite	17.5	0.3	0.32	32.4	3.79
Turii Peninsula massif						
GIM-3010	Nepheline pyroxenite	1552.0	9.8	0.24	10.6	5.26
GIM-3012	Nepheline pyroxenite	885.6	8.1	0.14	24.1	9.07
T-66	Olivine melteigite porphyry	24.9	1.72	<0.0335	16.8	5.46
GIM-4696	Turjaite	1054.7	28.0	1.1	6.6	2.34
T63	Turjaite	1303.5	12.6	0.29	24.6	8.86
Salma massif						
S-2011/13	Olivinite	88.6	3.3	0.55	2.3	4.27
S-2011/72	Olivinite	1154.0	19.3	0.17	86.4	6.3
S-2011/118.5	Olivinite	314.4	9.8	1.3	1.45	4.95
S-2011/183.3	Olivinite	557.2	51.2	6.3	18	1.67
S-2011/189.5	Olivinite	199.0	10.1	0.62	2.8	0.33
S-2011/189.5-ol	Olivine from olivinite	169.2	2.5	0.65	1.1	2.06
S-2011/189.5-mgt	Magnetite from olivinite	322.4	21.2	2.8	2.1	0.42
S-2011/191	Olivinite	441.8	25.9	1.17	6.9	1.29
S-2011/195	Mineralized olivinite	171.0	15.2	1.22	3.2	0.46
S-2011/199	Olivinite	99.5	3.7	0.46	1.9	1.69
S-2011/253.5	Olivinite	845.8	10.1	1.1	12.3	2.14
S-2011/304.5	Olivinite	597.0	8.0	0.29	7.2	3.84
S-2032/13	Mineralized olivinite	1910.4	8.1	0.26	4.6	4.82
S-2032/268	Olivinite	8457.5	114.2	3.3	21.5	6.67
S-201l/183.3-a	Pyroxenite	666.7	45.3	1.39	19.6	2.74
S-2011/184.5	Ijolite–urtite	1771.0	109.5	5.5	34.6	3.09
S-2011/199-a	Ijolite–urtite from vein in olivinites	4099.0	135.7	9.2	16.5	2.81
S-2015/349	Ijolite	11741.0	297.5	18.5	34.1	4.82
S-2031-2	Ijolite	2865.6	199.9	23.4	19.8	3.21
NSG-2030-5	Ijolite	96.5	1.3	<0.0335	13.0	1.75
S-11	Melteigite	606.95	29.8	1.85	9.3	3.28

Table 1. (Contd.)

Sample*	Rock (mineral)	HCG, $cm^3/g \times 10^{-6}$			^3He, cm^3/g $\times 10^{-12}$	R/Ra** ($^3He/^4He$)
		CH_4	C_2H_6	C_3H_8		
S-48	Ijolite	3681.5	351.6	61.4	8.0	1.71
S-19	Turjaite	726.4	37.5	2.4	56.5	4.54
S-2033/261	Turjaite	9054.5	211.8	12.1	353	4.52
S-2033/290	Turjaite	5870.5	240.4	22.4	245	3.37
Ozernaya Varaka massif						
OV-2048/117.4	Nepheline pyroxenite	23.1	1.44	0.87	23.6	0.88
OV-2048/118	Pyroxenite	20.7	1.02	0.24	38.2	2.07
OV-2050/302.8	Nepheline pyroxenite	16.3	0.94	0.24	18.5	1.29
OV-2050/302.8-pr	Pyroxene from pyroxenite	21.5	1.1	0.25	17.1	1.09
OV-2057/116	Nepheline pyroxenite	87.6	2.1	0.26	41.6	2.7
OV-2044/163.2	Ijolite	57.7	1.5	0.63	1.13	2.01
OV-2044/230	Ijolite	33.8	2.4	0.77	7.4	1.15
OV-2057/12	Ijolite urtite	13.5	0.4	0.45	7.3	1.3
OV-2057/212	Ijolite	17.9	1.05	0.49	9.8	1.67
NOV-2053-1	Ijolite	31.4	1.1	0.25	12.0	1.38

Notes: * Rock and minerals sampled from it have the same number. Samples from the Lesnaya Varaka and Turii Peninsula massifs were taken from natural outcrops. Most samples from other massifs are cores of prospecting boreholes. In the sample number, the numerator denotes the borehole, and the denominator indicates sampling depth in meters.

** Data on He isotope composition were taken as $^4He/^3He$ from [5] and recalculated to R/Ra, where R is the measured $^3He/^4He$, and Ra is the atmospheric ratio, Ra = 1.4×10^{-6} [4].

extracted gases, only those were analyzed that were present in most samples in amounts sufficient for quantitative determination. These components are saturated hydrocarbons: methane, ethane, and propane (CH_4, C_2H_6, and C_3H_8). The major component of hydrocarbon gases extracted from the rocks of all massifs is methane, ranging from 90.1 to 99.3% of total HCG with predominant values within 96–99%. The content of HCG strongly varies between the massifs and within an individual massif from 8.5 to 12057×10^{-6} cm^3/g (Table 1), and there is a positive correlation between CH_4 and the sum of $C_2H_6 + C_3H_8$ (Fig. 1). It can be seen that almost all samples from the massifs of Salma, Lesnaya Varaka, Sebljavr, and Turii Peninsula are located in the right part of the diagram, at elevated HCG contents. The data points of the Ozernaya Varaka massif and most samples from the Kovdor and Vuorijarvi massifs occur closer to the origin. Among the ultramafic rocks, the highest HCG contents were found in the olivinites of the Sebljarv massif, and, among the pyroxenites, the Vuorijarvi massif appeared to be richest in HCG. The highest HCG contents among the alkaline rocks were found in the ijolites–urtites of the Salma massif. The melilite rocks (turjaites and melilitites) of the Kovodor and Salma massifs are also characterized by elevated contents of HCG.

Data on the abundance and isotopic composition of helium in fluid inclusions from the samples were taken from [5], and He isotopic compositions were recalculated to R/Ra, where R is the measured $^3He/^4He$ value, and Ra is an atmospheric ratio of 1.4×10^{-6} [4]. R/Ra values and ^3He contents for all samples shown in diagrams are given in Table 1. These data show that the maximum values of R/Ra ratios in five of the seven massifs are higher than the upper mantle value (R/Ra = 8). The highest values were found in the Sebljarv massif, where all samples yielded R/Ra > 8. The lowest R/Ra ratios are typical of the Ozernaya Varaka massif.

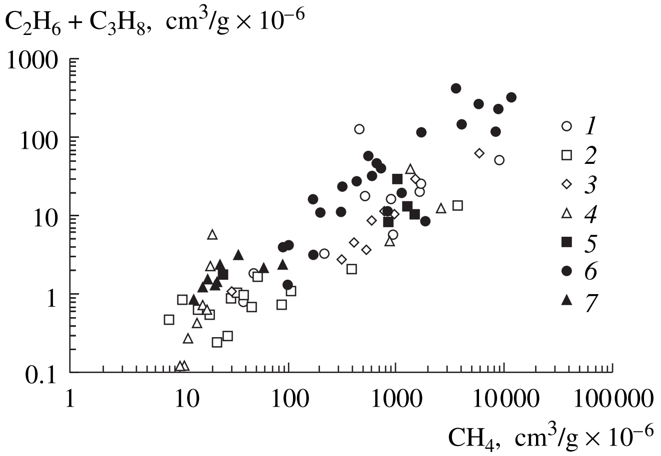

Fig. 1. Variations of methane (CH_4) versus heavy hydrocarbons (C_2H_6–C_3H_8). Massifs: (*1*) Sebljavr, (*2*) Kovdor, (*3*) Lesnaya Varaka, (*4*) Vuorijarvi, (*5*) Turii Peninsula, (*6*) Salma, and (*7*) Ozernaya Varaka.

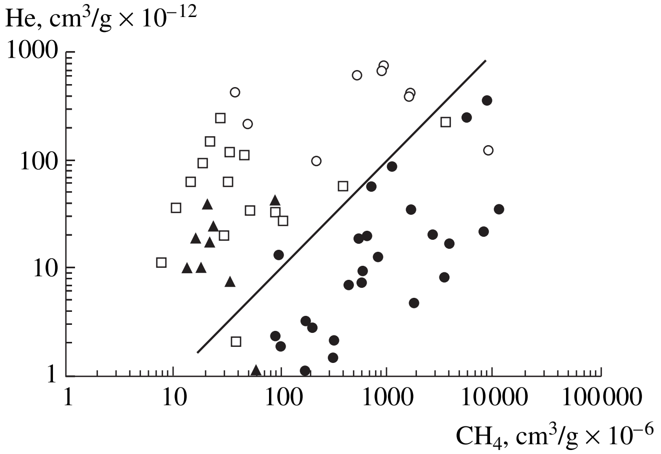

Fig. 2. Diagram of CH_4 versus ^3He. Symbols are the same as in Fig. 1.

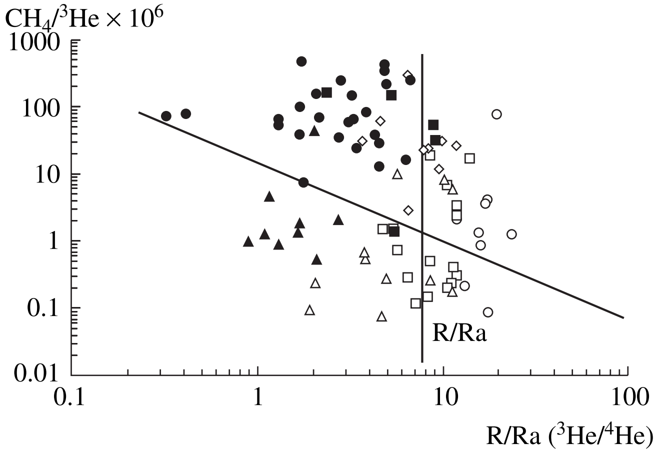

Fig. 3. Diagram of R/Ra($^3He/^4He$)–$CH_4/^3He$. See text for explanation, symbols are the same as in Fig. 1.

Assuming that all extracted and measured ^3He is of primary origin [5] and that the fluid phase of magmatic melts contained HCG, it is reasonable to expect a positive correlation between methane, the major HCG component, and ^3He. Such a comparison is shown in Fig. 2 for the Sebljavr and Kovdor massifs, where the maximum R/Ra values are 2–3 times higher than that of the upper mantle, and for the rocks from the Salma and Ozernaya Varaka massifs whose R/Ra ratios are lower than in the upper mantle (Table 1). The diagram of Fig. 2 exhibits a distinct positive correlation between CH_4 and ^3He for the rocks of the Salma massif. A combined set of analyses from the other three massifs also shows the same correlation with a parallel increase in ^3He and CH_4 contents.

When natural gases are investigated, for example, in subduction zones [15], in addition to a direct comparison of ^3He and CH_4 contents, the $CH_4/^3He$ ratio is used as an indicator of the contributions of mantle and crustal components in a mixed fluid. It is assumed that methane and ^3He in this ratio represent crustal and mantle sources, respectively. The appearance of methane in a fluid is attributed to the thermal decomposition of organic matter in the rocks of continental crust under the influence of ascending mantle melts. Carbon isotopic composition provides direct evidence for the crustal origin of HCG. Methane formed by the destruction of organic matter has $\delta^{13}C$ (relative to PDB) from –46 to –32 ‰ [15]. A mixed fluid enriched in mantle components is characterized by low $CH_4/^3He$ and elevated R/Ra ($^3He/^4He$) ratios. These parameters for the sample set studied are shown in Fig. 3. It can be seen that the diagonal line separates the samples into two fields, each showing a negative correlation between R/Ra and $CH_4/^3He$. The upper field contains data points for the massifs of Salma, Lesnaya Varaka, and Turii Peninsula and most points of the Sebljarv massif. The rocks of Ozernaya Varaka are plotted in the lower field, whereas samples from the Kovodor and Vuorijarvi massifs are plotted in both fields. The samples with R/Ra > 8, i.e., having ratios higher than the mantle value, show strongly varying $CH_4/^3He$ ratios (from 0.1×10^6 to 77×10^6), with predominant values of $(0.18–31) \times 10^6$ (right part in Fig. 3).

Based on numerous data on HCG composition from active hydrothermal vents in the areas of different tectonomagmatic settings, including hot spots (Iceland), Darling [16] proposed to use the CH_4/C_2H_6 ratio as an indicator of fluid temperature (t°C) determined by the formula

$$t°C = 57.8\log(CH_4/C_2H_6) + 96.8.$$

Figure 4 shows data for each massif in the CH_4/C_2H_6–R/Ra coordinates. It can be seen that the data for most massifs exhibit an increase in CH_4 /C_2H_6 with increasing R/Ra. This correlation is most distinct in the Vuorijarvi and Ozernaya Varaka massifs and least apparent in the Kovdor massif. Table 2 shows the temperature of HCG-bearing fluids calculated using the above formula. However, it must be taken into account that there

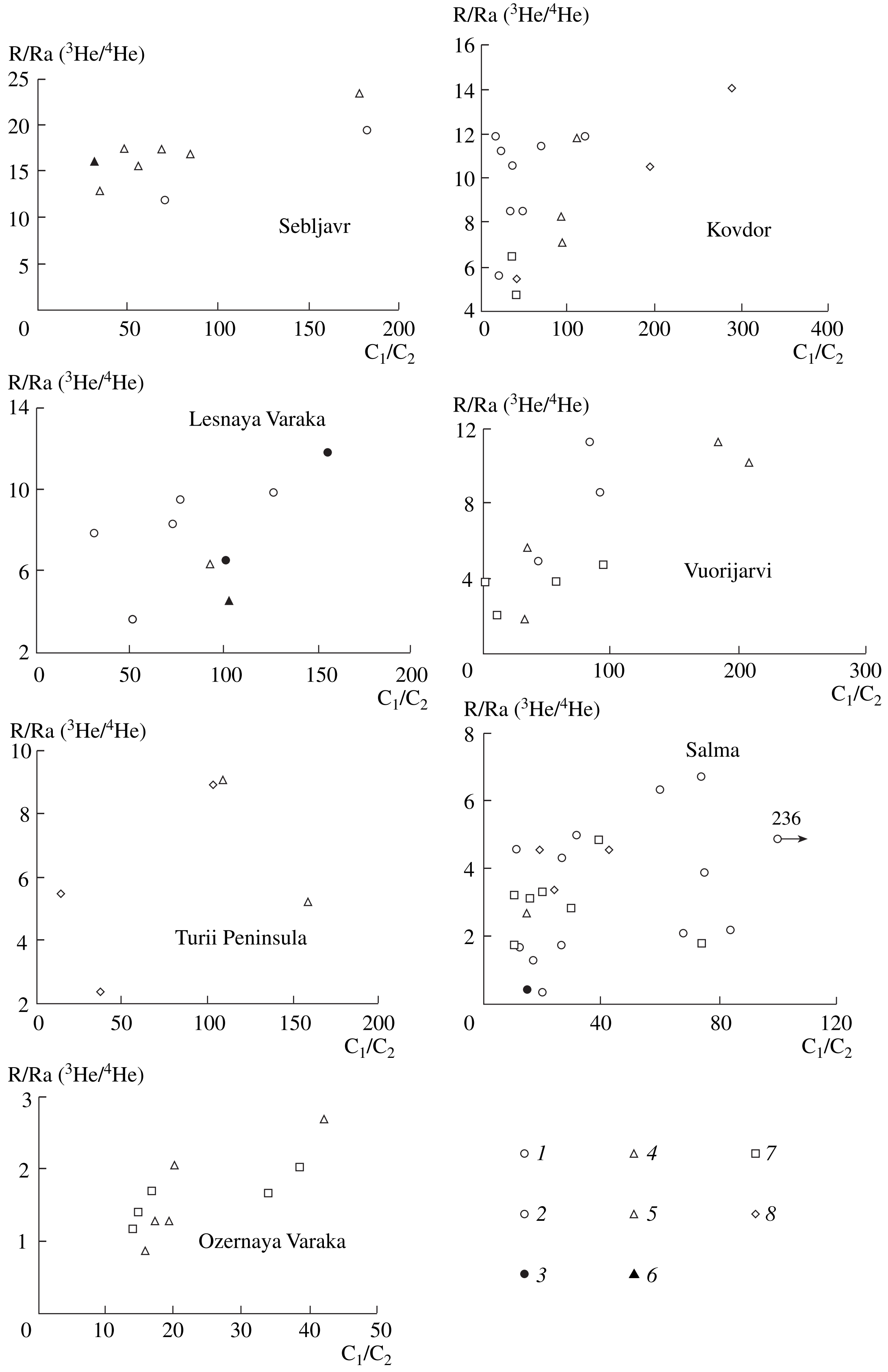

Fig. 4. Variations of methane to ethane ratio (C_1/C_2) versus R/Ra for each massif. (*1*) Olivinite, (*2*) olivine from olivinite, (*3*) magnetite from olivinite, (*4*) pyroxenite, (*5*) pyroxene from pyroxenite, (*6*) magnetite from pyroxenite, (*7*) ijolite–urtite, and (*8*) melilite.

Table 2. Temperatures of fluids calculated from the methane/ethane ratio for the rocks of the massif

Massif	Number of samples	Variations (t, °C)	Dominant range (t, °C)
Sebljavr	9	183.8–227.5	194.2–208.4
Kovdor	16	166.7–238.9	186.3–217.0
Lesnaya Varaka	9	183–218.2	196.0–210.6
Vuorijarvi	11	155.1–230.8	184.1–211.1
Turii Peninsula	5	163.9–223.9	188.1–214.6
Salma	25	155.8–234	164.8–191.2
Ozernaya Varaka	9	163.2–190.6	166.4–172.4

are significant differences between the thermodynamic conditions of the formation of fluids, for which this formula was developed, and those at the postmagmatic stage of the formation of alkaline–ultramafic intrusions. Therefore, the calculated temperatures can be considered only as possible evidence for comparatively low-temperature conditions of the formation and conservation of HCG inclusions in the massifs.

The obtained results do not provide compelling evidence for the input of HCG with mantle melts. Nonetheless, it can be concluded that CH_4 and other hydrocarbons could not be formed by thermal decomposition of organic matter from continental crustal rocks. This is indicated by the carbon isotopic compositions of HCG from the ijolite and ijolite–urtite of the Salma massif reported by E.M. Galimov. The measured $\delta^{13}C$ values (relative to PDB) were –16.0 and –16.1‰, respectively. Thus, the carbon isotopic composition of these samples shows significantly higher ^{13}C content compared with methane produced by the thermal decomposition of organic matter, and, at the same time, it is close to the isotopic composition of HCG from the rocks of the Khibiny alkaline massif [17]. Similar to the Khibiny massif, the HCG of the alkaline ultramafic rocks of the Kola Peninsula were presumably formed during a postmagmatic stage [11] owing to the interaction between H_2 and mantle carbon at relatively low temperatures, for example, following the mechanism proposed in [10]. The generated HCG were mixed with the fluid released from the melt during magmatic crystallization and were conserved as secondary inclusions in early minerals together with mantle-derived ^{3}He. The secondary origin of the fluid inclusions is supported, in particular, by the distribution of inclusions in nepheline from the Salma massif [8], where the highest HCG contents were determined. The significant variations in ^{3}He and HCG proportions, as well as in CH_4/C_2H_6 in the rocks of the massifs can be related to multiple episodes of HCG inclusion formation during the postmagmatic history of these alkaline–ultramafic intrusions. This process presumably spanned a significant temperature interval and occurred with different intensity within each massif.

ACKNOWLEDGMENTS

This work was supported by INTAS project no. 01–0244.

REFERENCES

1. F. P. Mitrofanov, S. V. Ikorsky, and I. L. Kamensky, “He Isotopes in the Paleozoic Alkaline Intrusions of the Kola Peninsula and Northern Karelia,” Dokl. Akad. Nauk **345**, 243–246 (1995).
2. S. V. Ikorsky, I. L. Kamensky, and V. A. Nivin, “Helium Isotopic Variations in the Paleozoic (380–360 Ma) Complexes of the Kola Alkaline Province: High^{3}He/^{4}He Ratios Are Signs of Devonian Mantle Plume?,” in *Proceedings of 9th Meeting of European Union of Geosciences, Strasbourg, France, 1997* (Strasbourg, 1997), p. 56.
3. T. B. Bayanova, V. I. Pozhilenko, V. F. Smol’kin, et al., *Catalogue of Geochronological Data for the Northeastern Baltic Shield*, Ed. by F. P. Mitrofanov (Geol. Inst. KNTs RAN, Apatity, 2002) [in Russian].
4. I. N. Tolstikhin and B. Marty, “The Evolution of Terrestrial Volatiles: A View from Helium, Neon, Argon and Nitrogen Isotope Modeling,” Chem. Geol. **147**, 27–52 (1998).
5. I. N. Tolstikhin, I. L. Kamensky, B. Marti, et al., *Identification of the Lower Mantle Plume Component in the Devonian Alkaline–Ultramafic Complexes of the Kola Peninsula on the Basis of Noble Gas Isotope Systematics* (Apatity, Nancy, and Brussels, 1999) [in Russian].
6. I. N. Tolstikhin, I. L. Kamensky, B. Marty et al., “Rare Gas Isotopes and Parent Trace Elements in Ultrabasic–Alkaline–Carbonatite Complexes, Kola Peninsula: Identification of Lower Mantle Plume Component,” Geochim. Cosmochim. Acta **66**, 881–901 (2002).
7. I. L. Kamensky, I. V. Sharkov, S. V. Ikorsky, et al., “Helium is Always an Admixture to Volatiles,” in *Alkaline Magmatism of the Earth* (GEOKhI RAN, Moscow, 2001), p. 38 [in Russian].
8. S. V. Ikorsky, V. A. Nivin, and V. A. Pripachkin, *Geochemistry of Gases in Endogenous Rocks* (Nauka, St. Petersburg, 1992) [in Russian].
9. R. Sugisaki and K. Mimura, “Mantle Hydrocarbons: Abiotic Or Biotic?,” Geochim. Cosmochim. Acta **58**, 2527–2542 (2002).
10. I. D. Ryabchikov, “Carbon Compounds under Upper Mantle Conditions,” Geokhimiya, No. 11, 1539–1546 (1988).
11. S. V. Ikorsky, “On the Distribution and Accumulation Time of Hydrocarbon Gases in the Rocks of the Khibiny Alkaline Massif,” Geokhimiya, No. 11, 1625-1634 (1977).

12. S. V. Ikorsky and A. S. Stepanova, “Apparatus for the Analysis of Gases from Microinclusions Extracted from Minerals by Sample Crushing,” Mineral. Zh. **12**, 88–91 (1990).
13. S. V. Ikorsky and I. L. Kamensky, “Technique of Crushing of Rocks and Minerals in Glass Ampoules for Noble Gases Isotope Studies,” in *Proceedings of 15th Symposium on Isotope Geochemistry, Moscow, Russia, 1998* (Moscow, 1998), p. 115 [in Russian].
14. A. A. Kukharenko, M. P. Orlova, A. G. Bulakh, et al., *Caledonian Complexes of Ultramafics, Alkaline Rocks, and Carbonatites of the Kola Peninsula and Northern Karelia* (Nedra, Moscow, 1965) [in Russian].
15. R. J. Poreda, A. W. A. Jeffrey, I. R. Kaplan, and H. Craig, “Magmatic Helium in Subduction Zone Natural Gases,” Chem. Geol. **71**, 199–210 (1988).
16. W. G. Darling, “Hydrothermal Hydrocarbon Gases: 1, Genesis and Geothermometry,” Appl. Geochem. **13**, 815–824 (1998).
17. E. M. Galimov and I. A. Petersil’e, “Carbon Isotope Composition of Hydrocarbon Gases and CO_2 form the Igneous Alkaline Rocks of the Khibiny, Lovozero, and Illimaussaq Massifs,” Dokl. Akad. Nauk SSSR **176**, 914–917 (1967).